Comparison of compressive forces generated with intramedullary nails using standard compression screws versus a magnetic compression device in a transverse tibial fracture model

Megan Audet MD[1], Dave Huang MS[1,2], Lauren Turner BS[1], Kelsey Bonilla MD[1], Geoffrey Marecek MD[1], Melodie F. Metzger PhD[1,2]

[1]Cedars-Sinai, Department of Orthopaedic Surgery, Los Angeles, CA [2]Cedars-Sinai Orthopaedic Biomechanics Laboratory, Los Angeles, CA

Melodie.Metzger@cshs.org

INTRODUCTION: Transverse tibial shaft fractures are challenging injuries with higher rates of reoperation and nonunion. Standard fixation with intramedullary nails provides relative stability, but transverse patterns require absolute stability achieved through compression. Several techniques such as dynamic interlocking, back-striking, compression screws, and supplemental plating, are used to minimize fracture gapping, though each has limitations. Even with these methods, delayed union and nonunion remain common, and exchange nailing often fails to resolve them. Magnetic lengthening nails, repurposed in reverse, offer a novel solution by providing continuous and adjustable compression across the fracture during healing. Prior biomechanical work shows these devices create greater and more uniform compression compared to standard plating, with the added advantage of titrating forces postoperatively. This study aimed to compare compression generated by a magnetic compression nail against a standard intramedullary nail with a compression screw, and to quantify the level of compression needed to stabilize transverse tibial fractures and promote bone healing.

METHODS: Twelve fourth-generation composite tibiae (Sawbone, 17 PCF solid foam core, medium) were divided into two groups of six: magnetic compression nail (MCN) versus standard intramedullary nail (IM) fixation. A controlled osteotomy was created at a standardized location, followed by nail implantation using the respective surgical technique. A Tekscan pressure mapping sensor (5051-2500), modified to accommodate the nail, was placed at the osteotomy site to measure interfragmentary compression. A silicone pad was interposed to protect the sensor surface, and the system was calibrated before each test using a standard five-point calibration procedure. After fixation, baseline compression was recorded, and specimens were potted in aluminum fixtures with epoxy and mounted in a biaxial hydraulic testing machine at 30° to simulate heel strike. Cyclic axial loading (400–1,000 N, 2 Hz, 14,400 cycles) was applied, with interfragmentary pressure recorded at baseline, mid-point, and end. MCNs were re-tightened at mid-point if pressures dropped below 20% of baseline. Following axial loading, specimens were reoriented perpendicular to the actuator for torsional testing (0.5–10 N·m internal rotation, 2 Hz, 14,400 cycles), with the same measurement protocol. Tibial deflection, rotation, and fracture-site contact parameters (area, force, mean and peak pressure) were continuously recorded.

RESULTS SECTION: During cyclic axial loading, both IM and MCN constructs demonstrated similar tibial deflection and interfragmentary pressure profiles. Deflection increased modestly from approximately 1.7–2.0 mm at 100 cycles to 2.0–2.4 mm at 14,400 cycles, with no statistically significant differences between groups at any time point (p > 0.05). Interfragmentary pressure also remained stable within each construct across the axial loading protocol, with baseline values near 3.7 MPa and no significant changes after 7,200 or 14,400 cycles. The MCN did not require re-tightening under axial loading conditions. In torsional loading, both groups experienced notable decreases in interfragmentary pressure, but only the MCN could regain compression following re-tightening. The IM group fell from 3.7 MPa initially to ~2.1 MPa after 7,200 and 14,400 cycles, with no recovery. The MCN followed a similar pattern, dropping to ~2.4 MPa at mid-point and ~2.3 MPa at endpoint, but pressures increased to ~3.5 MPa and ~3.3 MPa after re-tightening at 7,200 and 14,400 cycles, respectively. Statistical analysis confirmed no differences between IM and MCN in baseline or post-cycle states, but re-tightened MCN constructs demonstrated significantly higher pressures compared to both IM and loosened MCN (p < 0.05). Tekscan maps visually confirmed pressure loss with cycling and recovery after MCN re-tightening.

DISCUSSION: This study compared compressive stability of a MCN and an IM nail across a transverse tibial osteotomy under simulated loading. Both constructs performed similarly under axial loading with no significant differences in pressure or deflection. Under torsional loading, both lost ~60% of compression, but only the MCN restored forces after retightening, highlighting its advantage in maintaining stability and reducing risk of nonunion. These results align with prior work showing improved union when compression is augmented, including success with MCNs in nonunion cases. Slightly greater torsional deflection in the MCN likely reflects its telescoping design. Limitations include minor nail size differences, restricted MCN shortening during testing, and use of a synthetic bone model. Overall, the ability to restore compression dynamically makes the MCN a promising option for managing transverse tibial fractures and difficult nonunions.

SIGNIFICANCE/CLINICAL RELEVANCE: The ability to adjust compression postoperatively with an all-internal device may improve union rates and reduce the need for revision surgery, making MCNs a promising option for managing challenging long bone fractures.
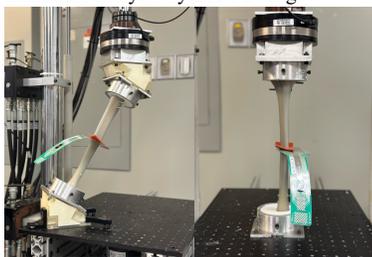
Figure 1. Experimental setup of tibial constructs under axial (left) and torsional load (right).
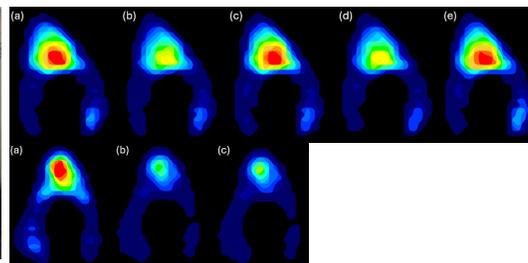

Figure 2. Tekscan pressure maps showing interfragmentary compression distribution for MCN (top row) and IM (bottom row) at baseline and after torsional cyclic loading.

Table 1. Interfragmentary pressure (MPa) for magnetic compression nail (MCN) versus standard intramedullary nail (IM) constructs across loading torsion cycles and retightening.

Condition	IM (MPa)	MCN (MPa)
Initial State	3.71 ± 0.68	3.64 ± 0.76
After 7200 Cycles	2.09 ± 0.94	2.36 ± 0.73
MN Retightening (Post-7200)	—	3.49 ± 0.65
After 14,400 Cycles	2.07 ± 0.91	2.34 ± 0.67
MN Retightening (Post-14400)	—	3.31 ± 0.86